3-D Molecular Assembly of Function in Titania-Based Composite Material Systems

MICHAEL H. BARTL,
SHANNON W. BOETTCHER,
KAREN L. FRINDELL, AND GALEN D. STUCKY*
Department of Chemistry & Biochemistry and California NanoSystems Institute, University of California at Santa Barbara, Santa Barbara, California 93106

Received June 22, 2004

ABSTRACT
Various examples of composite titania-based nanostructured materials exhibiting cooperative functionalities between different active components are presented. The fabrication of these integrated composite materials is based on one-pot supramolecular templating techniques combined with acidic sol−gel chemistry. The defined 3-D nanoscale organization and integration of various functional components results in advanced optoelectronic and photonic applications such as visible light sensitization of mesoporous titania photocatalysts with cadmium sulfide nanocrystals acting as sensitizing integral part of the mesopore wall structure, narrow bandwidth emission from rare earth ion activated nanocrystalline mesoporous titania films, and mirrorless lasing in dye-doped hybrid organic/inorganic mesostructured titania waveguides.

Introduction

One of the imposing technological challenges of the 21st century is to organize different functional components in three dimensions at the nanometer scale. For advanced optoelectronic and photonic applications that rely on controlled interactions between different functional units, such well-defined organization and integration of multiple active components is especially crucial. For example, photosynthesis—one of the most fundamental processes in biology—provides an excellent example of how the controlled interaction between functional subunits results in an efficiency-optimized integrated materials system. Photosynthetic organisms channel energy from light-harvesting outer units to a reaction center by transferring the excitation energy along multiple functional units with unity photon conversion efficiency for the overall process.[1] Ultimately, it is the cooperative interaction of different nanoscale components via transfer of energy, information, or both in the form of charge carriers, photons, spins, etc. that allows the combination of desirable properties of single units into a larger integrated system. While we are still far from achieving the efficient multifunctional systems developed by nature, complex nanostructured composites made by molecular or nanoparticle assembly can lead to interesting new and improved properties through the collective behavior of the functional units.[2,3] A number of successful strategies have been developed to fabricate 2- or 3-D nanostructured composite systems (see, e.g., refs 2−6 and references therein). Typical fabrication steps include synthesis and isolation of the functional nanounits, purification and surface modification of these building blocks, and finally their assembly into integrated higher order systems using a variety of techniques including, for example, colloidal self-assembly (for reviews, see, e.g., refs 3, 4, and 7), layer-by-layer assembly,[4,8,9] electrical assembly,[10] and programmed assembly through molecular recognition and bio-inspired routes.[11−16] In this Account, we will discuss an alternative approach for the fabrication of functional nanoscale material systems based on supramolecular templating/sol−gel chemistry that selectively utilizes competing molecular assembly, phase behavior, and condensation/crystallization processes. We show that this simple synthesis/assembly scheme can be applied to create various titania-based multicomposite materials exhibiting high nanoscale ordering and cooperative functionality of different active components.

Mesostructured Composites: 3-D Organization on the Nanoscale

The synergistic assembly capability of molecular organic and inorganic species has been recognized as a general and powerful approach for the fabrication of 3-D continuously ordered structures at length scales ranging from several angstroms to tens of nanometers.[17] While small molecules have been used to form zeolite-type microporous compounds with ordering lengths less than 3 nm,[18−21] this range was dramatically enlarged in the early 1990s with the discovery of so-called "mesostructured or mesoporous materials" fabricated through supramolecular assembly.[22,23] With surfactants or amphiphilic block co-

Michael H. Bartl was born in Radkersburg, Austria, in 1973. He received his Diploma degree (M.Sc.) in physical chemistry (2000) from the Graz University of Technology and his doctorate degree (Ph.D.) in chemistry (2002) from the Karl-Franzens-University of Graz under the direction of Professors Alois Popitsch and Galen Stucky. He conducted postdoctoral research at the University of California, Santa Barbara, as a Max-Kade-Foundation research fellow and is currently a postdoctoral member of the California NanoSystems Institute working with Professor Evelyn Hu. His research interests include nano- and microscale photonics and optoelectronics.

Shannon W. Boettcher was born in Santa Cruz, California, in 1981. He received his B.A. degree in chemistry from the University of Oregon, Eugene, and began his Ph.D. work with Professor Galen Stucky at the University of California, Santa Barbara, as a NSF graduate research fellow in 2003.

Karen L. Frindell was born in Bremerton, Washington, in 1976. She received her B.S. degree in chemistry (1998) from the University of California, Berkeley, and her Ph.D. in chemistry (2003) from the University of California, Santa Barbara, under the direction of Professor Galen Stucky. She is currently a Professor of Chemistry at Santa Rosa Junior College in Santa Rosa, California.

Galen D. Stucky was born in McPherson, Kansas, in 1936. He earned his B.S. degree (1957) from McPherson College and his Ph.D. degree with R. E. Rundle from Iowa State University in 1962. He held positions at the University of Illinois, Sandia National Laboratory, and DuPont Central Research and Development before joining the faculty of the University of California, Santa Barbara, in 1985, where he is Professor in the Department of Chemistry & Biochemistry and the Materials Department. His current research interests include synthesis and characterization of composite materials, understanding Nature's routes to organic/inorganic bio-assembly, and the chemistry associated with efficient utilization of energy resources.

* To whom correspondence should be addressed. E-mail: stucky@chem.ucsb.edu. Phone: 805-893-4872. Fax: 805-893-4120.

10.1021/ar040177o CCC: $30.25
Published on Web 04/02/2005

polymers as structure directing agents, ordered mesoporous materials with pore sizes ranging from 2 to 50 nm have been fabricated (see, e.g., refs 17, 19, 20, and 24 and references therein). Whereas the first synthetic efforts were directed toward silica-based materials for applications in sorption, separation, and catalysis,[25,26] it was soon realized that mesostructured silicas could also be used as hosts for a variety of functional guest species leading to novel applications including lasing, optical switching, and sensing (for reviews, see refs 27−30).

The discovery of transition metal oxide mesostructured materials with nanocrystalline semiconducting wall structures[31−33] was an important step toward inherently *functional* mesostructured compounds with potential uses as high-surface-area electrodes and optoelectronic devices.[19,34,35] Among these oxides, the wide-band-gap semiconductor titania is of particular interest, and different approaches to synthesize mesoporous titania have been developed over the past few years.[32,33,36−45] The major synthetic challenge is to introduce crystallinity into the framework while preserving the highly ordered mesostructural integrity of the material. In our group, we developed several surfactant-templated, sol−gel chemistry-based synthetic routes using (1) titanium tetrachloride in alcohol solvents,[32] (2) the acid/base reaction of titanium tetrachloride and titanium alkoxides in alcohol solvents,[45] and (3) the prehydrolysis of titanium alkoxides under strongly acidic aqueous conditions.[37,38] The key in these approaches is to nucleate high densities of nanocrystals within the amorphous framework walls. This partially crystalline wall structure sustains the local strain caused by the crystallization and prevents the mesostructure from collapsing. In all of these approaches, synthesis and processing can be combined to give crack-free, optically transparent titania films with cubic or hexagonal mesostructural ordering.

The materials described in this Account were fabricated using the third approach. In general, titanium alkoxide precursors are hydrolyzed in strong acids before they are combined with an ethanolic solution containing the mesostructure-directing nonionic block copolymer (e.g., Pluronic P123, a poly(ethylene oxide)$_{20}$−poly(propylene oxide)$_{70}$−poly(ethylene oxide)$_{20}$ triblock copolymer). From this solution, films are prepared by dip-coating onto appropriate substrates (glass slides, electrodes, etc.). Heat treatment of the films leads to the thermal removal of the polymeric structure-directing species and to the nucleation and growth of anatase nanocrystals. The final result is an ordered mesoporous film with a semiconducting two-phase wall structure composed of anatase nanocrystals and amorphous titania.[37]

In the following, we give three examples showing that this simple sol−gel synthesis scheme can readily be extended to create 3-D titania-based mesostructured materials with integrated active species such as cadmium chalcogenide nanocrystals, trivalent rare earth ions, and organic laser dyes. Furthermore, we will show that the nanoscale integration of these different active components results in cooperative optoelectronic and photonic functionalities based on sensitized charge separation, excitation/energy transfer, and optical amplification (Scheme 1).

Scheme 1. Schematic Energy Diagrams Showing Proposed Electron and Energy Transfer Mechanisms in Nanocrystalline Titania-Based Mesostructured Composites[a]

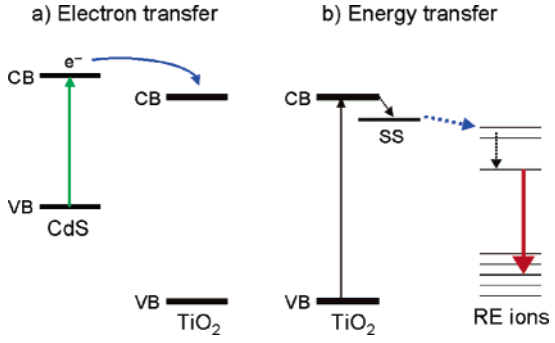

[a] (a) Sensitization of titania to visible light through electron transfer from CdS to anatase nanocrystals; (b) sensitized rare earth ion emission through energy transfer from UV light-harvesting anatase nanocrystals. VB = valence band; CB = conduction band; SS = surface state.

Cooperative Functionality in Mesostructured Composites

Integrated 3-D Arrays of Different Semiconductor Nanocrystals. Nanocrystalline anatase titania has proven to be an excellent candidate for use in low cost photocatalysis and solar energy conversion.[46] However, its large semiconductor band gap of 3.2 eV allows absorption of only the UV region of the solar spectrum resulting in low conversion efficiency. On the other hand, it has been shown that efficiency can be strongly increased through postsynthesis functionalization of titania with visible light-sensitizing species, for example, grafting of dye molecules or depositing narrow band gap semiconductor nanocrystals onto premade titania matrixes (Scheme 1a).[46−50] In contrast to these postsynthesis sensitization techniques, we developed a molecular templating/sol−gel chemistry-based synthesis for sensitized mesoporous titania that combines synthesis, assembly, and sensitization and results in cubic mesoporous frameworks with walls composed of integrated arrays of different types of wide and narrow band gap semiconductor nanocrystals (Figures 1 and 2).[51]

Mixed nanocrystalline anatase titania/cadmium chalcogenide mesoporous films were prepared by dip-coating from a single solution containing the hydrolyzed titania precursors, soluble cadmium salts, and the mesostructure-directing nonionic triblock copolymer (see ref 51 for synthesis details). The core of the fabrication process is an extended heat treatment of the dip-coated films under varying gas/vapor atmospheres. The films are first kept in an oxidative high-temperature environment to promote nucleation and growth of semiconducting anatase nanocrystals out of the amorphous titania matrix. Simultaneously, segregation of the coassembled cadmium species occurs into cadmium oxide nanoclusters distributed in the titania framework. By changing the processing conditions to an inert gas diluted sulfur (S) or selenium (Se) vapor

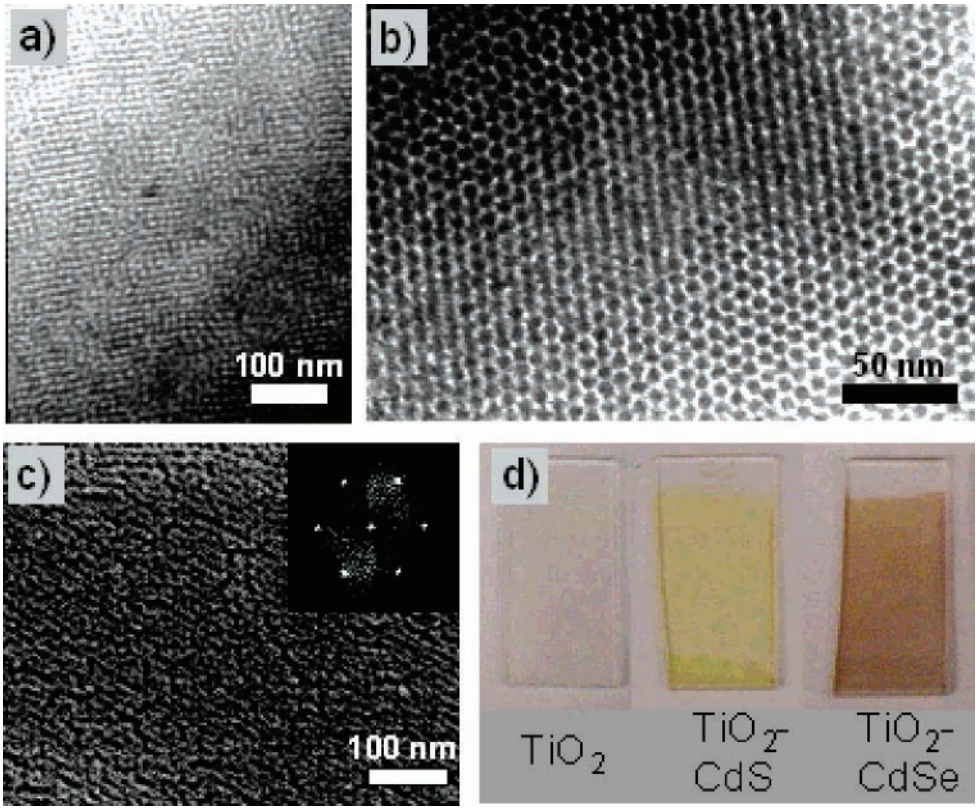

FIGURE 1. TEM images of mixed nanocrystalline titania/cadmium chalcogenide films recorded along the [100] (a) and [111] (b) zone axes of the *bcc* mesoporous symmetry, (c) SEM image and Fourier transform (inset) of the open-pore film surface, and (d) photographs of mesoporous pure titania and composite titania/cadmium chalcogenide films. Images are reproduced with permission from ref 51. Copyright 2004 Wiley.

atmosphere, we selectively convert the cadmium oxide nanoclusters into crystalline semiconducting CdS or CdSe nanoparticles through a redox-coupled ion exchange reaction mechanism.[52] After a few minutes of exposure to S and Se vapor, the films became visibly yellow or orange—indicating the successful transformation of cadmium oxide into its nanocrystalline sulfide or selenide analogue (Figure 1d).

Transmission electron microscopy (TEM) in combination with energy-dispersive X-ray spectroscopy (EDX) revealed that the films possess a highly ordered cubic (*bcc*) mesoporous structure with walls composed of titania and the respective cadmium chalcogenide phase (Figure 1a,b). High-resolution scanning electron microscopy (HR-SEM) indicates a completely open-pore film surface (Figure 1c) with the [111] direction of the *bcc* mesopore symmetry running perpendicular to the film surface, as indicated by the hexagonal Fourier pattern (inset in Figure 1c). This confirms that the cubic pore structure is extended throughout the film and fully accessible from the surface—an important feature, since it allows postsynthesis infiltration of the mesoporous framework with, for example, conjugated polymers.[53]

X-ray diffraction (XRD) analysis was used to investigate the titania and the cadmium chalcogenide phases. While the diffraction pattern of an undoped titania mesoporous film (pattern A in Figure 2) shows only the typical anatase reflections, the patterns obtained from samples doped with Cd and treated with either S or Se vapor (patterns B and C, respectively, in Figure 2) contain additional reflections that can all be assigned to the typical wurtzite structure of crystalline cadmium chalcogenides. The diffraction peaks are strongly broadened due to the small size of the anatase, CdS, and CdSe crystallites, which were estimated using the Scherrer formula to be between 4 and 7 nm.

To test for cooperative functionality, we analyzed the solar sensitization efficiency of nanocrystalline anatase/CdS mesoporous composite films by comparing their ability to generate a visible light photocurrent (I_{ph}) to that of pure anatase titania mesoporous films. A standard two-electrode photoelectrochemical cell working in nonregenerative mode was used for these measurements.[46] Measurements were done in two steps to eliminate fluctuations due to small sample and setup deviations (film thickness and surface roughness, angle of incident light). First, the I_{ph} response to UV and visible photons simultaneously (UV+vis) was determined. Since in this case both anatase and CdS are able to absorb light, this value was used as the maximal photoinducible I_{ph} under the given illumination. The sensitization effect to visible light, expressed as the I_{ph} response to visible photons only (vis-only), was then determined by blocking the UV photons with a 400 nm long-pass filter. Figure 3 gives typical results for pure anatase titania and anatase/CdS (5 mol % CdS) mesoporous films. As expected, for both samples a well-defined periodic on/off I_{ph} response to the light/dark modulated UV+vis illumination (violet background) was obtained. Under vis-only illumination (yellow background), however, no measurable I_{ph} was generated by the pure anatase

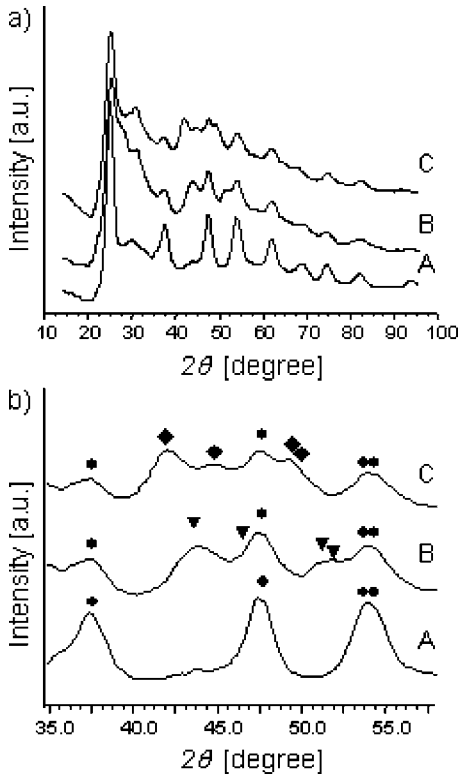

FIGURE 2. Offset XRD patterns (a) of nanocrystalline pure anatase titania (A) and anatase/CdS (B) and anatase/CdSe (C) samples and detailed comparison (b) in the range 35° to 58° 2θ. Dots indicate the anatase (004), (200), and (105/211) reflections; triangles and diamonds mark the (110), (103), (112), and (201) wurtzite reflections of CdS and CdSe nanocrystals, respectively. Data are reproduced with permission from ref 51. Copyright 2004 Wiley.

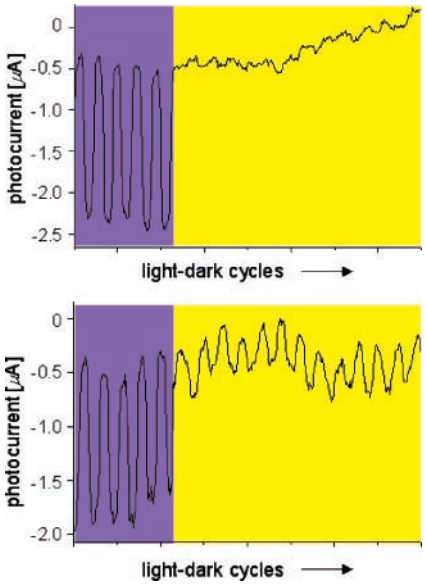

FIGURE 3. Periodic on/off photocurrent response curves of nanocrystalline pure anatase titania (a) and composite anatase/CdS (b) cubic mesoporous films illuminated with a periodically light/dark modulated xenon lamp. Violet background denotes illumination with UV and visible photons simultaneously. Yellow background denotes illumination with visible photons only. Data are reproduced with permission from ref 51. Copyright 2004 Wiley.

titania mesoporous films. In contrast, the composite anatase/CdS film produced a clear on/off I_{ph} response under vis-only illumination, which is around 25% of the total UV+vis I_{ph}. Considering that under vis-only excitation only the 5% CdS portion of the film is able to absorb photons, the conservation of 25% of the maximal photoinducible I_{ph} is exceptionally high and points to an efficient intrinsic visible light sensitization effect of the integrated CdS nanocrystals. Furthermore, we have recently shown that the optical density and the photocurrent generation in nanocrystalline mesostructured films can be respectively enhanced by fabricating homogeneous multilayer films (Bartl et al., unpublished) and by increasing the nanocrystallinity of the framework walls.[41] This makes these composite films promising components for low cost photovoltaic and photocatalytic applications.

Nanocrystals as Light-Harvesting Antennas for Sensitized Rare Earth Emission. The two-phase nanocrystalline/amorphous wall structure makes mesoporous titania an interesting host matrix for optically active inorganic species such as trivalent rare earth (RE^{3+}) ions, a technologically important class of narrow bandwidth emitters.[54,55] While the amorphous titania regions provide an ideal oxide glasslike environment for the incorporation of RE^{3+} ions, the UV light-harvesting nature of the wide band gap semiconductor anatase nanocrystals can sensitize RE^{3+} ion luminescence through indirect excitation pathways (Scheme 1b).[38,56,57] Sensitization is an important process for technological applications of RE^{3+} ions in photonic devices and color displays, since direct optical excitation of the parity forbidden intra-f-shell electronic transitions is rather inefficient.[58]

RE^{3+} ions can be doped into the two-phase nanocrystalline/amorphous framework of mesoporous titania thin films via the above-described sol−gel/supramolecular templating method by simply adding appropriate amounts of the rare earth ion chlorides to the titania precursor solution (for details, see refs 38 and 56). TEM and EDX studies show that RE^{3+} ion loadings as high as 10 mol % can be incorporated into the walls without destroying the cubic mesopore arrangement (Figure 4). Due to a large mismatch in ionic radii between RE^{3+} (>0.90 Å) and Ti^{4+} (0.68 Å) the RE^{3+} ions do not occupy titanium sites within the anatase nanocrystallites but rather sit close to their surface.

UV light excitation at 330 nm, well above the anatase nanocrystal band gap, of a trivalent europium (Eu^{3+})-doped mesoporous titania film results in strong red luminescence typical for Eu^{3+} ions, although Eu^{3+} has no crystal field absorption transition at this excitation wavelength.[58] The photoluminescence (PL) emission spectrum given in Figure 5b shows five characteristic Eu^{3+} bands between 550 and 720 nm arising from crystal field transitions between Russell−Saunders multiplets $^5D_0 \rightarrow {}^7F_J$ with $J = 0$, 1, 2, 3, and 4. All of the five transitions show strong inhomogeneous broadening, indicative of an amorphous environment. This is also confirmed by the PL lifetimes of the most intense $^5D_0 \rightarrow {}^7F_2$ electric dipole transition centered at 614 nm, which are 550, 520, 470, 500, and 330 μs for Eu^{3+} concentrations of 1, 3, 5, 8, and 10 mol % and

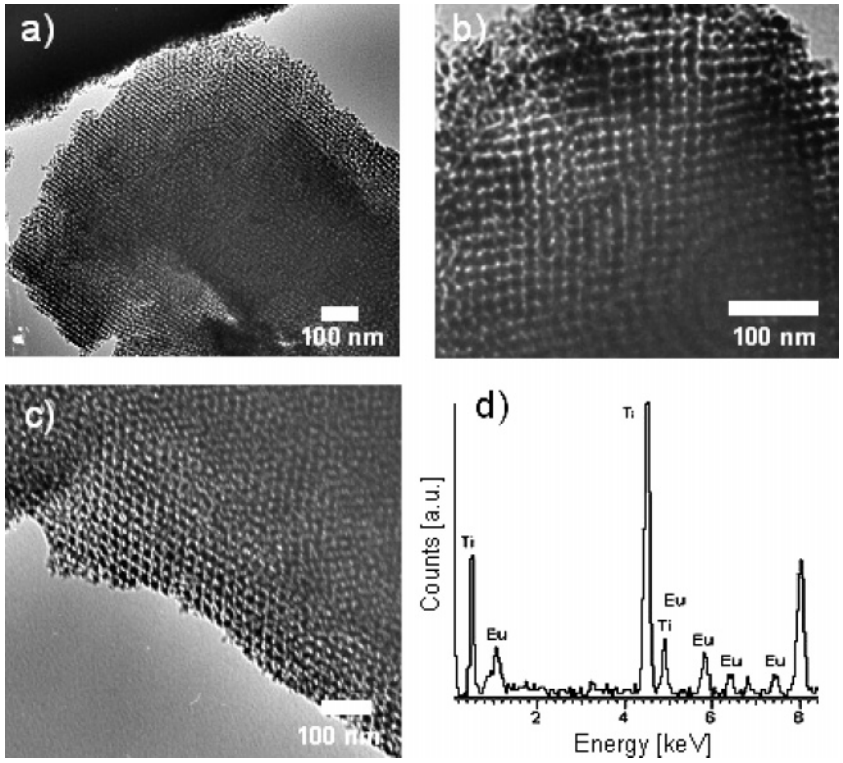

FIGURE 4. TEM images along the [100] zone axis (a, b) and down the [111] zone axis (c) and EDX spectrum (d) of 8 mol % Eu^{3+}-doped nanocrystalline anatase titania cubic mesoporous films. Images and data are reproduced with permission from ref 38. Copyright 2002 Wiley.

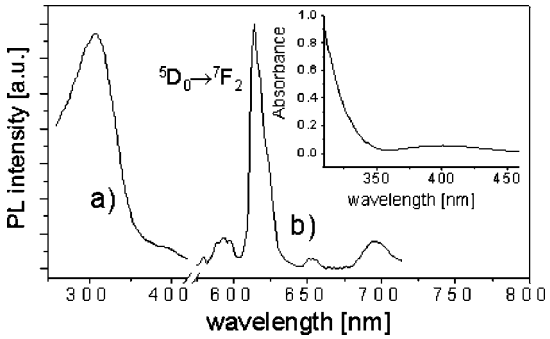

FIGURE 5. PL excitation (a) and emission (b) spectra of Eu^{3+}-activated nanocrystalline anatase titania mesoporous films. The inset shows the UV−vis absorption spectrum of the same sample. Data are reproduced with permission from ref 38. Copyright 2002 Wiley.

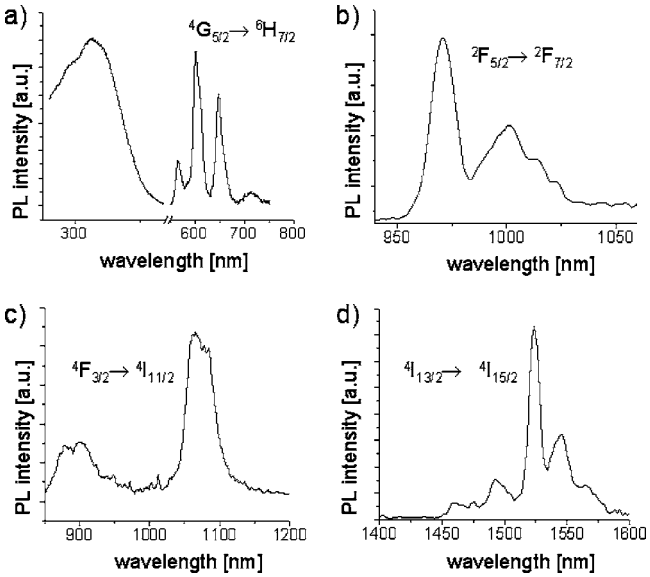

FIGURE 6. PL spectra of nanocrystalline anatase titania mesoporous films doped with samarium (a), ytterbium (b), neodymium (c), and erbium (d). All samples were excited at 325 nm. Data are reproduced with permission from ref 56. Copyright 2003 Elsevier.

compare well with results from other Eu^{3+}-doped sol−gel amorphous oxides.[59] However, in contrast to bulk oxide host matrixes, the PL lifetime in the mesoporous films stays constant at around 500 μs for Eu^{3+} contents of up to 8 mol %, which indicates that no PL concentration quenching occurs. We attribute this unique behavior to reduced clustering of the europium ions in this high surface and interface area mesoporous nanocrystalline/amorphous matrix.

We applied PL excitation spectroscopy to investigate the excitation pathway of the Eu^{3+} emission. The PL excitation spectrum of the $^5D_0 \rightarrow {}^7F_2$ emission band (Figure 5a) shows no Eu^{3+} crystal field transitions but exhibits only a broad peak starting at 360 nm and centered at 310 nm. This peak coincides very well with the absorption band edge of the anatase nanocrystals (inset in Figure 5) and clearly indicates that the Eu^{3+} luminescence is not the result of resonant excitation of europium crystal field transitions but is rather associated with an indirect excitation process. A detailed study of the sensitization mechanism was done by Frindell et al.,[56] who investigated the luminescence behavior of different RE^{3+} ions doped into mesoporous titania films (Figure 6). By comparing the crystal field energy levels of sensitized (samarium, ytterbium, neodymium, and erbium) and nonsensitized (thulium and terbium) RE^{3+} ions with the known conduc-

tion band and surface states energy positions of nanocrystalline anatase, one can conclude that the sensitized RE^{3+} emission process is the result of UV light absorption of the semiconducting anatase nanocrystals and subsequent relaxation to the nanocrystal surface states, followed by nonradiative energy transfer to crystal field states of the RE^{3+} ions located at the surface of the nanocrystals (Scheme 1b). Apart from revealing the energy transfer mechanism, these studies also expand the range of sensitized narrow bandwidth RE^{3+} emission from visible to the near-infrared including the technologically important region around 1550 nm.

Activated Nanohybrid Organic/Inorganic Titania Composites. The development of soft chemistry routes, that is, room-temperature synthesis, involving hydrolysis and condensation of inorganic precursors coupled with molecular self-assembly, has enabled advanced optical applications through the fabrication of activated hybrid mesostructured silica compounds (for reviews, see, e.g., refs 27−29). However, the low refractive index of hybrid silica composites ($n = 1.43$) limits their applications, since it requires that the optically active layer be supported by an ultralow refractive index layer such as mesoporous SBA-15 ($n = 1.15$)[60] for efficient waveguiding to occur. This limitation is overcome by a new synthesis and processing approach for the preparation of optically activated, high refractive index hybrid organic/inorganic mesostructured materials based on a titania inorganic framework.[61,62]

The fabrication of hybrid nanocomposites for optical applications via evaporation induced self-assembly (EISA)[63] requires controlling the chemistry of the structure-directing molecules and the framework-forming inorganic species simultaneously in the precursor solution. The inorganic species needs to be soluble long enough to allow for surfactant-directed mesophase assembly, but at the same time, it should also be able to stabilize the desired morphology by forming a solid, glasslike material of high optical quality at room temperature. Unfortunately, conventional routes to titania-based mesostructured materials that use, or in-situ generate, strong inorganic acids are limited to the fabrication of thin films that require additional heat treatment for stabilization.[37−41] We found, however, that by introducing trifluoroacetic acid (TFA) as a stabilizing ligand for reactive titanium alkoxides, the precursor solution can readily be processed at room temperature into glasslike, optically transparent morphologies. These include crack-free fibers and films with adjustable thickness from hundreds of nanometers to tens of micrometers and a high degree of mesostructural order (see Figure 7).[61]

The chemical interactions between TFA, the titanium alkoxide, and the structure-directing surfactants are critical in the formation of this material. First, TFA forms strong bidentate bridging or chelating coordination complexes with the titanium alkoxides in solution (Boettcher et al., submitted for publication). The small amount of added aqueous concentrated HCl hydrolyzes ethoxy groups on the TFA−titania complex, resulting in hydrophilic species with enhanced affinity to the hydrophilic block

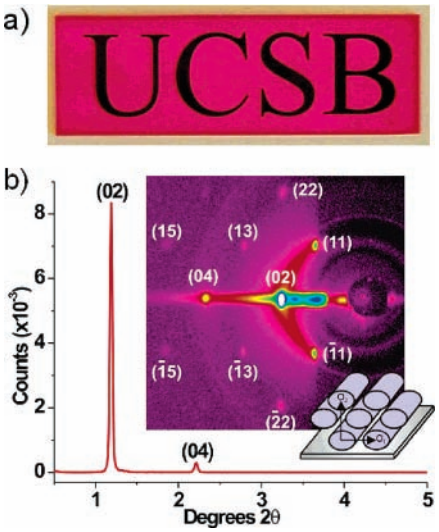

FIGURE 7. Optical photograph (a) of a 10 μm thick, R6G-doped hybrid mesostructured titania film deposited onto a glass slide lying atop the UCSB logo and (b) XRD and 2-D-SAXS (inset) pattern (collected at an incident angle of 0.4° and depicted on a false-color log scale) showing the 2-D hexagonal mesostructural order. The transmitted beams are blocked by the substrate. Data are reproduced with permission from ref 61. Copyright 2004 American Chemical Society.

of the surfactant template upon the EISA process. Furthermore, in contrast to HCl, which evaporates over time, a portion of the chelating TFA molecules remains permanently incorporated into the inorganic phase, controlling cross-linking and extended Ti−O bond formation in the mesopore walls giving a glasslike framework (see ref 61 for synthesis details).

Whereas the ability to actively control the macroscopic shape of the final product is an essential requirement for optical applications, the outlined organic/inorganic nanodomain separation in this material is the key for performance enhancement of incorporated organic dye emitters. While the inorganic titania-based framework raises the apparent index of refraction for the emitted light and enables efficient waveguiding, the organic nanodomains provide a chemically ideal environment for organic dyes. The dye molecules are homogeneously dispersed and therefore less prone to aggregate into nonluminescent dimers, which in turn yields high photoluminescence (PL) quantum efficiencies.[64]

Figure 8 shows PL emission spectra of a 1.5 wt % rhodamine 6G (an organic dye abbreviated as R6G)-doped, 10 μm thick mesostructured titania film excited by the second harmonic of a Q-switched Nd:YAG laser (532 nm, 10 ns pulse width, 10 Hz repetition rate). The laser was focused at a position around 5−10 mm away from the cleaved edge of the film, and the emitted light was collected in a 90° angle and analyzed by a spectrometer in combination with a CCD detector. Emission was recorded in two film orientations to better investigate the effect of waveguiding (see insets in Figure 8). While in "normal" 45° orientation, the typical broad R6G emission peak centered at around 585 nm is observed (top spectrum), turning the film into a 90° orientation, where

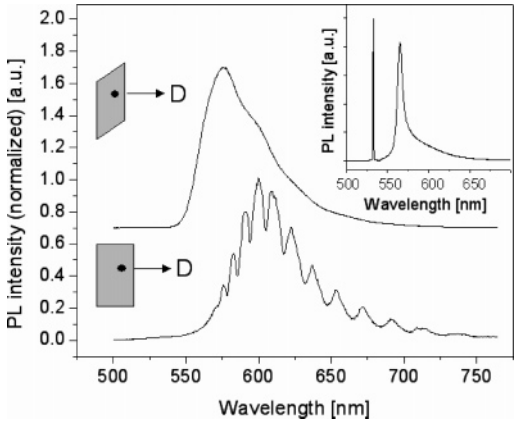

FIGURE 8. PL emission spectra showing "normal" emission (top) and waveguided emission (bottom) of a R6G-doped, 10 μm thick mesostructured titania film (film orientations are given at left). The inset shows the emission spectrum of the same sample above ASE threshold. The sharp line at 532 nm is scattered light from the excitation laser. Data are reproduced with permission from ref 61. Copyright 2004 American Chemical Society.

primarily waveguided photons are collected by the detector, the R6G emission peak is strongly modified and split into several well-defined modes (bottom spectrum). The spacings follow the theoretical formula for the free spectral range between adjacent waveguided modes, $\nu_{fsr} = c/(n2t)$ (c is the speed of light, n is the refractive index, and t is the film thickness).[65]

The waveguiding ability of dye-activated mesostructured titania films deposited directly onto glass substrates can be utilized for amplified spontaneous emission (ASE). ASE is a mirrorless lasing process, where, after exceeding a certain gain threshold, spontaneously emitted light is amplified by stimulated emission as it propagates along a waveguide containing the gain medium.[66] For ASE measurements, the excitation spot was moved closer to the film edge (1−2 mm) and the excitation power was slowly increased. Exceeding a certain threshold of the pump pulse energy (0.8−15 mJ depending on the film thickness and R6G dye concentration) resulted in mode competition and finally in the collapse of the multiple mode structure into a single, fully gain narrowed mode with a fwhm value of around 8−10 nm (Figure 8 inset), a typical signature of ASE.[66] It is important to note that for the mesostructured titania host, ASE of R6G was readily observed for films deposited directly onto glass slides, conditions under which mesostructured silica films, because of their low refractive index, fail to produce ASE. The higher refractive index of titania-based mesostructures therefore eliminates the need of a low refractive index support layer and facilitates integration into advanced optical structures.

Conclusions

Multicompositional mesostructured titania is an attractive material for a variety of optoelectronic and photonic applications. We have presented novel approaches for the simultaneous synthesis, 3-D organization, and integration of different functional species. The developed fabrication procedures are based on molecular templating strategies combined with simple one-pot sol−gel chemistry techniques. Highly ordered mesostructured samples can be prepared as either multiple-phase activated nanocrystalline frameworks or hybrid organic/inorganic high refractive index composites. We demonstrated that in both cases the defined 3-D nanoscale arrangement of different functional units enables their constructive interaction and results in material systems with cooperative functionalities such as in-situ solar sensitization, sensitized narrow bandwidth emission, and low threshold mirrorless lasing. Given the generality and flexibility of sol−gel self-assembly chemistry, the fabrication approach presented here opens the field to a multitude of new functional materials besides titania[32,45,67] with custom-made nanostructures and compositions.

We thank Stefan P. Puls, Jing Tang, Prof. Eric W. McFarland, and Prof. Evelyn L. Hu for valuable contributions. M.H.B. acknowledges the Austrian Academy of Sciences for a Max-Kade Postdoctoral Research Fellowship and the California NanoSystems Institute for financial support. S.W.B. thanks the NSF for a Graduate Research Fellowship. This material is based upon work supported by the NSF under Award DMR-02-33728 and the ARO under Contract Number DAAD19-03-D-0004, and made use of MRL Central Facilities supported by the MRSEC Program of the NSF under Award DMR-00-80034.

References

(1) Orrit, M. Photosynthesis − Coherent Excitation in the Antenna Complex. *Science* **1999**, *285*, 349−350.
(2) Alivisatos, A. P.; Barbara, P. F.; Castleman, A. W.; Chang, J.; Dixon, D. A.; Klein, M. L.; McLendon, G. L.; Miller, J. S.; Ratner, M. A.; Rossky, P. J.; Stupp, S. I.; Thompson, M. E. From Molecules to Materials: Current Trends and Future Directions. *Adv. Mater.* **1998**, *10*, 1297−1336.
(3) Liz-Marzan, L. M.; Norris, D. J.; Special Issue on: New Aspects of Nanocrystal Research. *MRS Bull.* **2001**, *26*, 981−984.
(4) *Colloids and Colloid Assemblies*; Caruso, F., Ed.; Wiley-VCH: Weinheim, Germany, 2003.
(5) Whitesides, G. M.; Grzybowski, B. Self-Assembly at All Scales. *Science* **2002**, *295*, 2418−2421.
(6) Colfen, H.; Mann, S. Higher-Order Organization by Mesoscale Self-Assembly and Transformation of Hybrid Nanostructures. *Angew. Chem., Int. Ed.* **2003**, *42*, 2350−2365.
(7) Murray, C. B.; Kagan, C. R.; Bawendi, M. G. Synthesis and Characterization of Monodisperse Nanocrystals and Close-Packed Nanocrystal Assemblies. *Annu. Rev. Mater. Sci.* **2000**, *30*, 545−610.
(8) Decher, G. Fuzzy Nanoassemblies: Toward Layered Polymeric Multicomposites. *Science* **1997**, *277*, 1232−1237.
(9) Kotov, N. A.; Dekany, I.; Fendler, J. H. Layer-by-Layer Self-Assembly of Polyelectrolyte-Semiconductor Nanoparticle Composite Films. *J. Phys. Chem.* **1995**, *99*, 13065−13069.
(10) Velev, O. D. Assembly of Electrically Functional Microstructures from Colloidal Particles. In *Colloids and Colloid Assemblies*; Caruso, F., Ed.; Wiley-VCH: Weinheim, 2003; pp 437−464.
(11) Cha, J. N.; Bartl, M. H.; Wong, M. S.; Popitsch, A.; Deming, T. J.; Stucky, G. D. Microcavity Lasing from Block Peptide Hierarchically Assembled Quantum Dot Spherical Resonators. *Nano Lett.* **2003**, *3*, 907−911.
(12) Hartgerink, J. D.; Beniash, E.; Stupp, S. I. Self-Assembly and Mineralization of Peptide-Amphiphile Nanofibers. *Science* **2001**, *294*, 1684−1688.
(13) Loweth, C. J.; Caldwell, W. B.; Peng, X. G.; Alivisatos, A. P.; Schultz, P. G. DNA-Based Assembly of Gold Nanocrystals. *Angew. Chem., Int. Ed.* **1999**, *38*, 1808−1812.

(14) Mirkin, C. A.; Letsinger, R. L.; Mucic, R. C.; Storhoff, J. J. A DNA-Based Method for Rationally Assembling Nanoparticles into Macroscopic Materials. *Nature* **1996**, *382*, 607−609.

(15) Whaley, S. R.; English, D. S.; Hu, E. L.; Barbara, P. F.; Belcher, A. M. Selection of Peptides with Semiconductor Binding Specificity for Directed Nanocrystal Assembly. *Nature* **2000**, *405*, 665−668.

(16) Tian, Z. R. R.; Voigt, J. A.; Liu, J.; McKenzie, B.; McDermott, M. J. Biomimetic Arrays of Oriented Helical ZnO Nanorods and Columns. *J. Am. Chem. Soc.* **2002**, *124*, 12954−12955.

(17) Stucky, G. D.; Huo, Q.; Firouzi, A.; Chmelka, B. F.; Schacht, S.; Voigt-Martin, I. G.; Schüth, F. Directed Synthesis of Organic/Inorganic Composite Structures. In *Progress in Zeolite and Microporous Materials, Studies in Surface Science and Catalysis*; Chon, H., Ihm, S.-K., Uh, Y. S., Eds.; Elsevier: Amsterdam, 1997; pp 3−28.

(18) Davis, M. E.; Lobo, R. F. Zeolite and Molecular-Sieve Synthesis. *Chem. Mater.* **1992**, *4*, 756−768.

(19) Soler-Illia, G. J. D.; Sanchez, C.; Lebeau, B.; Patarin, J. Chemical Strategies to Design Textured Materials: From Microporous and Mesoporous Oxides to Nanonetworks and Hierarchical Structures. *Chem. Rev.* **2002**, *102*, 4093−4138.

(20) Schüth, F.; Schmidt, W. Microporous and Mesoporous Materials. *Adv. Mater.* **2002**, *14*, 629−638.

(21) Zheng, N. F.; Bu, X. G.; Wang, B.; Feng, P. Y. Microporous and Photoluminescent Chalcogenide Zeolite Analogs. *Science* **2002**, *298*, 2366−2369.

(22) Yanagisawa, T.; Shimizu, T.; Kuroda, K.; Kato, C. The Preparation of Alkyltrimethylammonium-Kanemite Complexes and Their Conversion to Microporous Materials. *Bull. Chem. Soc. Jpn.* **1990**, *63*, 988−992.

(23) Kresge, C. T.; Leonowicz, M. E.; Roth, W. J.; Vartuli, J. C.; Beck, J. S. Ordered Mesoporous Molecular Sieves Synthesized by a Liquid-Crystal Template Mechanism. *Nature* **1992**, *359*, 710−712.

(24) Brinker, C. J. Porous Inorganic Materials. *Curr. Opin. Solid State Mater. Sci.* **1996**, *1*, 798−805.

(25) Corma, A. From Microporous to Mesoporous Molecular Sieve Materials and Their Use in Catalysis. *Chem. Rev.* **1997**, *97*, 2373−2419.

(26) Ying, J. Y.; Mehnert, C. P.; Wong, M. S. Synthesis and Applications of Supramolecular-Templated Mesoporous Materials. *Angew. Chem., Int. Ed.* **1999**, *38*, 56−77.

(27) Scott, B. J.; Wirnsberger, G.; Stucky, G. D. Mesoporous and Mesostructured Materials for Optical Applications. *Chem. Mater.* **2001**, *13*, 3140−3150.

(28) Wirnsberger, G.; Bartl, M. H.; Scott, B. J.; Stucky, G. D. Mesostructured Optical Devices by Room-Temperature Self-Assembly. *Aust. J. Chem.* **2001**, *54*, 225−227.

(29) Marlow, F. Optical Materials Based on Nanoscaled Guest/Host Composites. *Mol. Cryst. Liq. Cryst.* **2000**, *341*, 1093−1098.

(30) Davis, M. E. Ordered Porous Materials for Emerging Applications. *Nature* **2002**, *417*, 813−821.

(31) Huo, Q. S.; Margolese, D. I.; Ciesla, U.; Feng, P. Y.; Gier, T. E.; Sieger, P.; Leon, R.; Petroff, P. M.; Schüth, F.; Stucky, G. D. Generalized Synthesis of Periodic Surfactant Inorganic Composite Materials. *Nature* **1994**, *368*, 317−321.

(32) Yang, P. D.; Zhao, D. Y.; Margolese, D. I.; Chmelka, B. F.; Stucky, G. D. Generalized Syntheses of Large-Pore Mesoporous Metal Oxides with Semicrystalline Frameworks. *Nature* **1998**, *396*, 152−155.

(33) Khushalani, D.; Dag, O.; Ozin, G. A.; Kuperman, A. Glycometallate Surfactants. Part 2: Non-Aqueous Synthesis of Mesoporous Titanium, Zirconium and Niobium Oxides *J. Mater. Chem.* **1999**, *9*, 1491−1500.

(34) Behrens, P. Voids in Variable Chemical Surroundings - Mesoporous Metal Oxides. *Angew. Chem., Int. Ed. Engl.* **1996**, *35*, 515−518.

(35) Sanchez, C.; Soler-Illia, G.; Ribot, F.; Grosso, D. Design of Functional Nano-Structured Materials Through the Use of Controlled Hybrid Organic−Inorganic Interfaces. *C. R. Chim.* **2003**, *6*, 1131−1151.

(36) Antonelli, D. M. Synthesis of Phosphorus-Free Mesoporous Titania via Templating with Amine Surfactants. *Microporous Mesoporous Mater.* **1999**, *30*, 315−319.

(37) Alberius, P. C. A.; Frindell, K. L.; Hayward, R. C.; Kramer, E. J.; Stucky, G. D.; Chmelka, B. F. General Predictive Syntheses of Cubic, Hexagonal, and Lamellar Silica and Titania Mesostructured Thin Films. *Chem. Mater.* **2002**, *14*, 3284−3294.

(38) Frindell, K. L.; Bartl, M. H.; Popitsch, A.; Stucky, G. D. Sensitized Luminescence of Trivalent Europium by Three-Dimensionally Arranged Anatase Nanocrystals in Mesostructured Titania Thin Films. *Angew. Chem., Int. Ed.* **2002**, *41*, 959−962.

(39) Grosso, D.; Soler-Illia, G.; Babonneau, F.; Sanchez, C.; Albouy, P. A.; Brunet-Bruneau, A.; Balkenende, A. R. Highly Organized Mesoporous Titania Thin Films Showing Mono-Oriented 2D Hexagonal Channels. *Adv. Mater.* **2001**, *13*, 1085−1090.

(40) Crepaldi, E. L.; Soler-Illia, G.; Grosso, D.; Cagnol, F.; Ribot, F.; Sanchez, C. Controlled Formation of Highly Organized Mesoporous Titania Thin Films: From Mesostructured Hybrids to Mesoporous Nanoanatase TiO_2. *J. Am. Chem. Soc.* **2003**, *125*, 9770−9786.

(41) Tang, J.; Wu, Y.; McFarland, E. W.; Stucky, G. D. Synthesis and Photocatalytic Properties of Highly Crystallized and Ordered Mesoporous TiO_2 Thin Films. *Chem. Commun.* **2004**, 1670−1671.

(42) Hwang, Y. K.; Lee, K. C.; Kwon, Y. U. Nanoparticle Routes to Mesoporous Titania Thin Films. *Chem. Commun.* **2001**, 1738−1739.

(43) Yun, H. S.; Miyazawa, K.; Zhou, H. S.; Honma, I.; Kuwabara, M. Synthesis of Mesoporous Thin TiO2 Films with Hexagonal Pore Structures Using Triblock Copolymer Templates. *Adv. Mater.* **2001**, *13*, 1377−1380.

(44) Wang, Y. Q.; Tang, X. H.; Yin, L. X.; Huang, W. P.; Hacohen, Y. R.; Gedanken, A. Sonochemical Synthesis of Mesoporous Titanium Oxide with Wormhole-Like Framework Structures. *Adv. Mater.* **2000**, *12*, 1183−1186.

(45) Tian, B. Z.; Liu, X. Y.; Tu, B.; Yu, C. Z.; Fan, J.; Wang, L. M.; Xie, S. H.; Stucky, G. D.; Zhao, D. Y. Self-Adjusted Synthesis of Ordered Stable Mesoporous Minerals by Acid−Base Pairs. *Nat. Mater.* **2003**, *2*, 159−163.

(46) Grätzel, M. Photoelectrochemical Cells. *Nature* **2001**, *414*, 338−344.

(47) Nozik, A. J. Quantum Dot Solar Cells. *Physica E* **2002**, *14*, 115−120.

(48) Hagfeldt, A.; Grätzel, M. Molecular Photovoltaics. *Acc. Chem. Res.* **2000**, *33*, 269−277.

(49) Vogel, R.; Hoyer, P.; Weller, H. Quantum-Sized PbS, CdS, Ag2S, Sb2S3, and Bi2S3 Particles as Sensitizers for Various Nanoporous Wide-Band gap Semiconductors. *J. Phys. Chem.* **1994**, *98*, 3183−3188.

(50) Plass, R.; Pelet, S.; Krueger, J.; Grätzel, M.; Bach, U. Quantum Dot Sensitization of Organic−Inorganic Hybrid Solar Cells. *J. Phys. Chem. B* **2002**, *106*, 7578−7580.

(51) Bartl, M. H.; Puls, S. P.; Tang, J.; Lichtenegger, H. C.; Stucky, G. D. Cubic Mesoporous Frameworks with a Mixed Semiconductor Nanocrystalline Wall Structure and Enhanced Sensitivity to Visible Light. *Angew. Chem., Int. Ed.* **2004**, *43*, 3037−3040.

(52) Dloczik, L.; Engelhardt, R.; Ernst, K.; Fiechter, S.; Sieber, I.; Konenkamp, R. Hexagonal Nanotubes of ZnS by Chemical Conversion of Monocrystalline ZnO Columns. *Appl. Phys. Lett.* **2001**, *78*, 3687−3689.

(53) Coakley, K. M.; McGehee, M. D. Photovoltaic Cells Made from Conjugated Polymers Infiltrated into Mesoporous Titania. *Appl. Phys. Lett.* **2003**, *83*, 3380−3382.

(54) Steckl, A. J.; Zavada, J. M. Special Issue on: Photonic Applications of Rare-Earth-Doped Materials. *MRS Bull.* **1999**, *24*, 16−20.

(55) Maas, H.; Currao, A.; Calzaferri, G. Encapsulated Lanthanides as Luminescent Materials. *Angew. Chem., Int. Ed.* **2002**, *41*, 2495−2497.

(56) Frindell, K. L.; Bartl, M. H.; Robinson, M. R.; Bazan, G. C.; Popitsch, A.; Stucky, G. D. Visible and Near-IR Luminescence via Energy Transfer in Rare Earth Doped Mesoporous Titania Thin Films with Nanocrystalline Walls. *J. Solid State Chem.* **2003**, *172*, 81−88.

(57) Conde-Gallardo, A.; Garcia-Rocha, M.; Hernandez-Calderon, I.; Palomino-Merino, R. Photoluminescence Properties of the Eu3+ Activator Ion in the TiO2 Host Matrix. *Appl. Phys. Lett.* **2001**, *78*, 3436−3438.

(58) Hüfner, S. *Optical Spectra of Transparent Rare Earth Compounds*; Academic Press: New York, 1978.

(59) Lochhead, M. J.; Bray, K. L. Spectroscopic Characterization of Doped Sol−Gel Silica-Gels and Glasses − Evidence of Inner-Sphere Complexation of Europium(III). *J. Non-Cryst. Solids* **1994**, *170*, 143−154.

(60) Yang, P. D.; Wirnsberger, G.; Huang, H. C.; Cordero, S. R.; McGehee, M. D.; Scott, B.; Deng, T.; Whitesides, G. M.; Chmelka, B. F.; Buratto, S. K.; Stucky, G. D. Mirrorless Lasing from Mesostructured Waveguides Patterned by Soft Lithography. *Science* **2000**, *287*, 465−467.

(61) Bartl, M. H.; Boettcher, S. W.; Hu, E. L.; Stucky, G. D. Dye-Activated Hybrid Organic/Inorganic Mesostructured Titania Waveguides. *J. Am. Chem. Soc.* **2004**, *126*, 10826−10827.

(62) Vogel, R.; Meredith, P.; Kartini, I.; Harvey, M.; Riches, J. D.; Bishop, A.; Heckenberg, N.; Trau, M.; Rubinsztein-Dunlop, H. Mesostructured Dye-Doped Titanium Dioxide for Micro-Optoelectronic Applications. *ChemPhysChem* **2003**, *4*, 595−603.

(63) Brinker, C. J.; Lu, Y. F.; Sellinger, A.; Fan, H. Y. Evaporation-Induced Self-Assembly: Nanostructures Made Easy. *Adv. Mater.* **1999**, *11*, 579−585.
(64) Bartl, M. H.; Scott, B. J.; Wirnsberger, G.; Popitsch, A.; Stucky, G. D. Single-Photon Hot Band Absorption Induced Anti-Stokes Luminescence of Rhodamine 101 in Mesostructured Thin Films. *ChemPhysChem* **2003**, *4*, 392−395.
(65) *Fundamentals of Photonics*; Saleh, B. E. A., Teich, M. C., Eds.; Wiley: New York, 1991.
(66) Siegman, A. E. *Lasers*; University Science Books: Mill Valley, CA, 1986.
(67) Yang, P.; Deng, T.; Zhao, D.; Feng, P.; Pine, D.; Chmelka, B. F.; Whitesides, G. M.; Stucky, G. D. Hierarchically Ordered Oxides. *Science* **1998**, *282*, 2244−2246.

AR040177O